UW-CPTC 09-2

Note on Kinetic Alfvén Waves

February 9, 2009
(Revised February 27, 2009)

Carl R. Sovinec

University of Wisconsin-Madison
Department of Engineering Physics

This work is supported by U.S. Dept. of Energy Award Numbers DE-FC02-08ER54975 and DE-FG02-06ER54850.

Note on Kinetic Alfvén Waves

Carl Sovinec, University of Wisconsin-Madison

February 9, 2009

Like the whistler wave, the kinetic Alfvén wave (KAW) is dispersive, and its response is considered to be an important part of two-fluid magnetic reconnection when there is a large guide field [1-2]. The description in Ref. [1] refers to standing-wave behavior. One can envision that when field-lines reconnect, the point of reconnection is like the point of a guitar string that has been pulled and is about to be released. In the reconnection process, the field-lines do not oscillate back and forth, but the dynamics immediately after reconnection is similar to the fraction of a standing-wave period that follows the maximum magnetic-field phase. It is argued that with phase speed proportional to wavenumber, these dispersive waves are able to sweep magnetic flux out of arbitrarily small reconnection layers [1]. The two-fluid reconnection process does not suffer from the choking that occurs with constant phase-speed MHD.

Unlike the whistler, pressure evolution is critical in KAW dynamics. Even with relatively simple fluid models, pressure changes the differential order of the system. When deriving dispersion relations assuming a uniform background and complex-exponential basis functions, the characteristic equation becomes high order, and finding the KAW is nontrivial. Here, we will identify a couple of simplifying approximations to show a derivation that is relatively straightforward. We will use this approximation to find information about the KAW eigenvector and hence the physics of this mode. We will also compare the model with the low-frequency MHD limit and then consider how the transition is represented in more complete models.

The dispersion relations plotted in Fig. 1 have been obtained numerically with the DISPERSION code, keeping all terms in a fluid model. With the logarithmic scales, traces for all non-dispersive waves have the same slope, and traces for all $\omega\sim k^2$ waves have twice the slope of all $\omega\sim k$ waves. Comparing nearly parallel propagation (Fig. 1a) with nearly perpendicular propagation (Fig. 1b), we see that among the three low-frequency branches, the whistler is the dispersive wave for parallel propagation, but the KAW is the dispersive wave for nearly perpendicular propagation. For nearly parallel propagation at small plasma-β, the shear Alfvén mode starts transitioning to the L-mode ion-cyclotron resonance ($\omega=\Omega_i$), but when the frequency of the sound wave approaches the shear mode, there is another transition for both modes. Ion response in the medium-frequency branch becomes unmagnetized in the sense that the wave oscillation is faster than the gyro-period, so the gyro-motion becomes unimportant for the ions.

For nearly perpendicular propagation, the cyclotron resonance is down-shifted by $\cos(\theta)$, where θ is the angle between the wavenumber vector $\mathbf{k}$ and the background magnetic field. The magnetization aspect of the ion motion for the medium-frequency wave also loses importance at lower frequency, and this leads to the transition from shear Alfvén to KAW. The dispersion relation through the transition is necessarily complicated, but we can see that the KAW continues above the ion cyclotron frequency. This suggests that the KAW dispersion relation at higher frequencies can be obtained by ignoring $q_i\mathbf{v}_i\times\mathbf{B}_0$ force. With frequencies well below electron plasma and cyclotron frequencies, we can also ignore electron inertia. One more simplification in the analytics here is that all thermal energy is in the electrons. Ion-FLR effects would formally be needed otherwise.

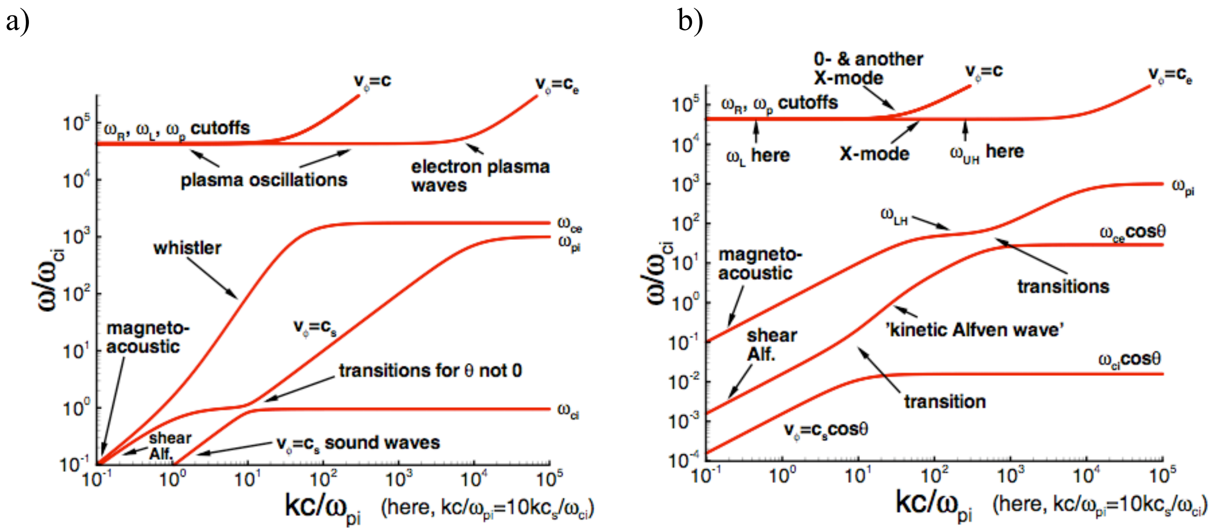

a) Dispersion relation for the full warm plasma model with the parameters of Swanson's Fig. 3.1. V_A/c_s=10, c/V_A=1000, m_i/m_e=1836, and ω_{pe}/ω_{ce}=23.3, except θ=π/10 for nearly parallel propagation. Electron fluid pressure effects are used without further approximation. Here, p_{i0}=0 and γ_e=1.

b) Dispersion relation for the full warm plasma model with the parameters of Swanson's Fig. 3.1. V_A/c_s=10, c/V_A=1000, m_i/m_e=1836, and ω_{pe}/ω_{ce}=23.3, except θ=0.495π for nearly perpendicular propagation. Electron fluid pressure effects are used without further approximation. Here, p_{i0}=0 and γ_e=1.

Figure 1. Numerically obtained dispersion relations for the warm plasma model for a) nearly parallel propagation and b) nearly perpendicular propagation.

We will use the common plane-wave setup of orienting the background magnetic field, $\mathbf{B}_0$ in the z-direction, $\mathbf{k}$ is in the x-z plane, and the background electrons and ions have no net flow. There is also no background electric field. With the approximations given above, and assuming plane-wave $e^{i\mathbf{k}\cdot\mathbf{x}-i\omega t}$ dependence of the perturbed fields, the equations for the perturbed ion flow simplify to

$$-i\omega\mathbf{v}_i = \frac{q_i}{m_i}\mathbf{E} \tag{1}$$

where $\mathbf{E}$ is the perturbed electric field. From this point, we will use q_i=e, so the two species have the same background number density (n_0). Without inertia, the electron equation of motion is

$$0 = -en_0\left(\mathbf{E} + \mathbf{v}_e \times \hat{\mathbf{z}}B_0\right) - i\,\mathbf{k}p_e\ . \tag{2}$$

With adiabatic electrons, the perturbed electron pressure obeys

$$\omega p_e = \gamma P_0 \mathbf{k}\cdot\mathbf{v}_e\ . \tag{3}$$

Combining Eqs. (2) and (3) in component form, we have

$$
\begin{aligned}
0 &= -en_0\left(E_x + v_{e_y}B_0\right) - i\frac{\gamma P_0}{\omega}k_x\left(k_x v_{e_x} + k_z v_{e_z}\right) \\
0 &= -en_0\left(E_y - v_{e_x}B_0\right) \\
0 &= -en_0E_z - i\frac{\gamma P_0}{\omega}k_z\left(k_x v_{e_x} + k_z v_{e_z}\right)
\end{aligned} \quad . \tag{4}
$$

The second equation of (4) implies that the x-component of electron motion is simply $\mathbf{E}\times\mathbf{B}_0$ drift. Defining $\Pi \equiv \gamma P_0/m_e n_0 = \gamma v_{th}^2/2$ and using $\Omega_e = eB_0/m_e$, we can solve for the following relations for electron velocity:

$$
\begin{aligned}
v_{e_x} &= \frac{e}{m_e\Omega_e}E_y \\
v_{e_y} &= \frac{e}{m_e\Omega_e}\left(-E_x + \frac{k_x}{k_z}E_z\right) \\
v_{e_z} &= \frac{e}{m_e}\left(-\frac{k_x}{k_z\Omega_e}E_y + i\frac{\omega}{\Pi k_z^2}E_z\right)
\end{aligned} \tag{5}
$$

Equations (1) and (5) will be used to find charge-current density; they effectively identify a conductivity through $\mathbf{J} = \underline{\underline{\sigma}}\cdot\mathbf{E} = en_0\left(\mathbf{v}_i - \mathbf{v}_e\right)$.

Our wave equation results from the combination of Faraday's law and Ampere's law, dropping displacement current as part of a low-frequency approximation. Using the plane-wave spatial dependence in the wave equation produces

$$
\left(k^2\mathbf{I} - \mathbf{kk}\right)\cdot\mathbf{E} = i\mu_0\omega\mathbf{J} \quad , \tag{6}
$$

and with the effective conductivity from the equations of motion, we have the following homogeneous algebraic equation:

$$
\begin{pmatrix}
k_z^2 + d_i^{-2} & i\dfrac{\omega}{d_e^2\Omega_e} & -k_x k_z \\
-i\dfrac{\omega}{d_e^2\Omega_e} & k^2 + d_i^{-2} & i\dfrac{\omega}{d_e^2\Omega_e}\dfrac{k_x}{k_z} \\
-k_x k_z & -i\dfrac{\omega}{d_e^2\Omega_e}\dfrac{k_x}{k_z} & k_x^2 + d_i^{-2} - \dfrac{\omega^2}{d_e^2\Pi k_z^2}
\end{pmatrix}
\cdot
\begin{pmatrix} E_x \\ E_y \\ E_z \end{pmatrix}
=
\begin{pmatrix} 0 \\ 0 \\ 0 \end{pmatrix} \quad , \tag{7}
$$

where species skin-depths are $d_\alpha = c/\omega_\alpha$ and species plasma frequencies are $\omega_\alpha = \sqrt{n_0 q_\alpha^2/\varepsilon_0 m_\alpha}$.

At this point, it is helpful to recall that coupling of x- and y-components is strictly from $\mathbf{E}\times\mathbf{B}_0$ motion of the electrons. Coupling of the y- and z-components is more complicated. Compression of flow along **k**, which includes $\mathbf{E}\times\mathbf{B}_0$ drift, couples with electric field via the adiabatic electron pressure through the z-component (parallel to $\mathbf{B}_0$) of force-balance, as represented by the third equation of (4). The perturbed pressure is also coupled to the y-component of electron motion through the x-component of the force balance, the first equation of

(4). This equation shows that the y-component of electron flow is a combination of $\mathbf{E}\times\mathbf{B}_0$ and diamagnetic drifts.

With the square of the skin depth proportional to mass, and the gyrofrequency inversely proportional to mass, we can use $d_e^2\Omega_e = d_i^2\Omega_i$ in the off-diagonal terms of Eq. (7). Multiplying all rows of (7) by d_i^2, normalizing frequency by the ion cyclotron frequency ($\underline{\omega}\equiv\omega/\Omega_i$), and normalizing wavenumber by ion skin depth ($\underline{k}\equiv k\,d_i$) simplifies the matrix:

$$\begin{pmatrix} \underline{k}_z^2+1 & i\underline{\omega} & -\underline{k}_x\underline{k}_z \\ -i\underline{\omega} & \underline{k}^2+1 & i\underline{\omega}\dfrac{\underline{k}_x}{\underline{k}_z} \\ -\underline{k}_x\underline{k}_z & -i\underline{\omega}\dfrac{\underline{k}_x}{\underline{k}_z} & \underline{k}_x^2+1-\dfrac{\underline{\omega}^2}{\beta\underline{k}_z^2} \end{pmatrix}\cdot\begin{pmatrix} E_x \\ E_y \\ E_z \end{pmatrix}=\begin{pmatrix} 0 \\ 0 \\ 0 \end{pmatrix} . \tag{8}$$

The β defined here is c_s^2/c_A^2 and appears from the relations $c_s^2=\Pi m_e/m_i$ and $c_A=d_i\Omega_i$. The determinant of a matrix of this Hermitian form simplifies:

$$\det\begin{pmatrix} A & iB & -C \\ -iB & D & iE \\ -C & -iE & F \end{pmatrix}=FAD+2BEC-AE^2-DC^2-FB^2 , \tag{9}$$

and for the system (8), the characteristic equation is

$$\underline{\omega}^4-\left[\left(1+\underline{k}^2\right)\left(1+\underline{k}_z^2\right)+\beta\underline{k}^2\right]\underline{\omega}^2+\beta\underline{k}_z^2\left(1+\underline{k}^2\right)^2=0 . \tag{10}$$

No limits have been used so far, but recall that we ignore electron inertia and assume cold unmagnetized ions. These approximations limit the dispersion relation to quadratic in $\underline{\omega}^2$.

Equation (10) is solved with the quadratic formula, but the square-root term is messy without taking limits. For nearly parallel propagation, where $\underline{k}_z^2\cong\underline{k}^2$, we can arrange the discriminant into $\left[\left(1+\underline{k}^2\right)\left(1+\underline{k}_z^2\right)-\beta\underline{k}^2\right]^2+4\beta\underline{k}_x^2\left(1+\underline{k}^2\right)$ and use $\beta\underline{k}_x^2$ as a small factor. Keeping just the large term leads to the two approximate solutions

$$\underline{\omega}^2\cong\begin{cases}\left(1+\underline{k}^2\right)\left(1+\underline{k}_z^2\right) , & \text{'+' solution} \\ \beta\underline{k}^2 , & \text{'−' solution}\end{cases} . \tag{11}$$

The '+' branch is the dispersive, right circularly polarized whistler wave, and the '−' branch is the demagnetized sound wave at $\underline{k}^2>>1$ (see Fig. 1a). For nearly perpendicular propagation, we can use $\beta\underline{k}_z^2<<1$ in (10) to find

$$\underline{\omega}^2 \cong \begin{cases} \left(1+\underline{k}^2\right)\left(1+\underline{k}_z^2\right)+\beta\underline{k}^2 & , \quad \text{'+' solution} \\ \dfrac{\beta\underline{k}_z^2\left(1+\underline{k}^2\right)^2}{\left(1+\underline{k}^2\right)\left(1+\underline{k}_z^2\right)+\beta\underline{k}^2} & , \quad \text{'−' solution} \end{cases} \quad . \tag{12}$$

Here, the '+' branch is the compressional Alfvén (CA) wave (what Ref. [3] calls 'magnetoacoustic' at low frequency, in contrast to Ref. [2]) that continues without dispersion at $\underline{\omega}^2 \cong (1+\beta)\underline{k}^2$ for $\underline{k}_z^2 << 1$ and $\underline{k}^2 >> 1$ (Fig. 1b). Its electric-field polarization rotates between the **k** and $\mathbf{B}_0\times\mathbf{k}$ directions ($E_y \cong iE_x/\underline{k}\sqrt{1+\beta}$) with a small parallel component, $E_z \cong E_x\underline{k}_z\beta/\underline{k}(1+\beta)$. [See the discussion for the KAW polarization below, and for the CA polarization, $\underline{k}_z$ is treated as a small parameter in the matrix.]

The '−' solution of (12) is the KAW (see Fig. 1b). For $\underline{k}_z^2 << 1$ and wavelengths that are small relative to the ion skin depth ($\underline{k}^2 >> 1$), which is necessarily the case for this mode with our restriction on frequencies, the dispersion relation further simplified to

$$\underline{\omega}^2 \cong \frac{\beta}{1+\beta}\underline{k}_z^2\underline{k}^2 \quad \text{or} \qquad \omega^2 \cong \frac{c_s^2 c_A^2}{c_A^2+c_s^2}k_z^2 k^2 d_i^2 \tag{13}$$

in agreement with Eq. (8) of Ref. [1]. Using this relation and $\underline{k}_x \cong \underline{k}$ in Eq. (8),

$$\begin{pmatrix} 1 & i\sqrt{\dfrac{\beta}{1+\beta}}\underline{k}\underline{k}_z & -\underline{k}\underline{k}_z \\ -i\sqrt{\dfrac{\beta}{1+\beta}}\underline{k}\underline{k}_z & \underline{k}^2 & i\sqrt{\dfrac{\beta}{1+\beta}}\underline{k}^2 \\ -\underline{k}\underline{k}_z & -i\sqrt{\dfrac{\beta}{1+\beta}}\underline{k}^2 & \dfrac{\beta}{1+\beta}\underline{k}^2-\underline{k}_z^2 \end{pmatrix}\cdot\begin{pmatrix} E_x \\ E_y \\ E_z \end{pmatrix} \cong \begin{pmatrix} 0 \\ 0 \\ 0 \end{pmatrix} , \tag{14}$$

helps us identify the eigenmodes. If β is not too small, we can also ignore the $-\underline{k}_z^2$ in the *zz*-element of the matrix. The third row is approximately $-i\sqrt{\beta/1+\beta}$ times the second row to order $\underline{k}_z/\underline{k}$. This suggests the phase relation

$$E_y \cong -i\sqrt{\frac{\beta}{1+\beta}}E_z \quad . \tag{15}$$

Using (15) in the first row of (14) produces

$$E_x \cong \frac{1}{1+\beta} \underline{k}\underline{k}_z E_z \quad . \tag{16}$$

This does not satisfy the second and third rows exactly, but with $\underline{k}_z^2 << 1$, it is an approximate solution for the eigenvector.

To verify this approximate dispersion relation and polarization, we compare with a KAW eigenmode generated by the DISPERSION code for the full warm plasma model and parameters of $\underline{k} = 19.6$, $\underline{k}_z = 0.31$, and $\beta = 0.64$. The computation is similar to the KAW shown in Fig. 1b, except that β is much larger, which makes E_y comparable to E_z in magnitude. The frequency computed from DISPERSION is $\underline{\omega} = 3.27$, whereas Eq. (13) predicts 3.77. Also, DISPERSION produces $E_x/E_z = 3.0$ and $E_y/E_z = -0.65i$, whereas Eqs. (16) and (14) predict 3.7, and -0.62i, respectively. The polarization information from the DISPERSION calculation is also displayed in Fig. 2. As time increases, the phase angle decreases at a fixed location, so the components of **E** that are perpendicular to **k** rotate in the right-handed sense. There is also a larger electrostatic component of **E** that is parallel to **k**.

To understand the dispersive nature of the KAW, it is helpful to draw an analogy with the more familiar whistler wave with **k** nearly parallel to $\mathbf{B}_0$. At frequencies above the ion cyclotron frequency, there is no ion drift motion, so $\mathbf{E} \times \mathbf{B}_0$ electron drift leads to net charge current density, and this is the dominant contribution to charge current in the whistler. The upper-left 2×2 submatrix of (8) produces the $\omega \sim k^2$ dispersion relation and the circular polarization about **k** with E_x leading E_y.

Tilting the **k**-vector to be nearly in the x-direction for the KAW, we have elliptical polarization in the y-z plane with E_y leading E_z. Considering Eq. (4) and the discussion following Eq. (7), electron $\mathbf{E} \times \mathbf{B}_0$ drift from E_y is coupled to the compressive flow that leads to pressure perturbations, and pressure perturbations couple with E_z through force-balance parallel to $\mathbf{B}_0$. Substituting the KAW dispersion (13) into just the zz-element of (8) makes the lower-right 2×2 submatrix of (8) look similar to the whistler submatrix with k^2 terms on the diagonal and ω^1 terms on the off-diagonal. The critical role of electron $\mathbf{E} \times \mathbf{B}_0$ drift in the $\omega \sim k^2$ dispersion is similar to the whistler. What's different is the coupling with pressure and the potentially significant E_x. With the approximations used in (14) to find (16), E_x generates ion current in the x-direction from unmagnetized acceleration parallel to **E**. For the electrons, the discrepancy between the electric-field and pressure forces in this direction is balanced by the Lorentz force, hence there is a combination $\mathbf{E} \times \mathbf{B}_0$ and diamagnetic drifts in the y-direction.

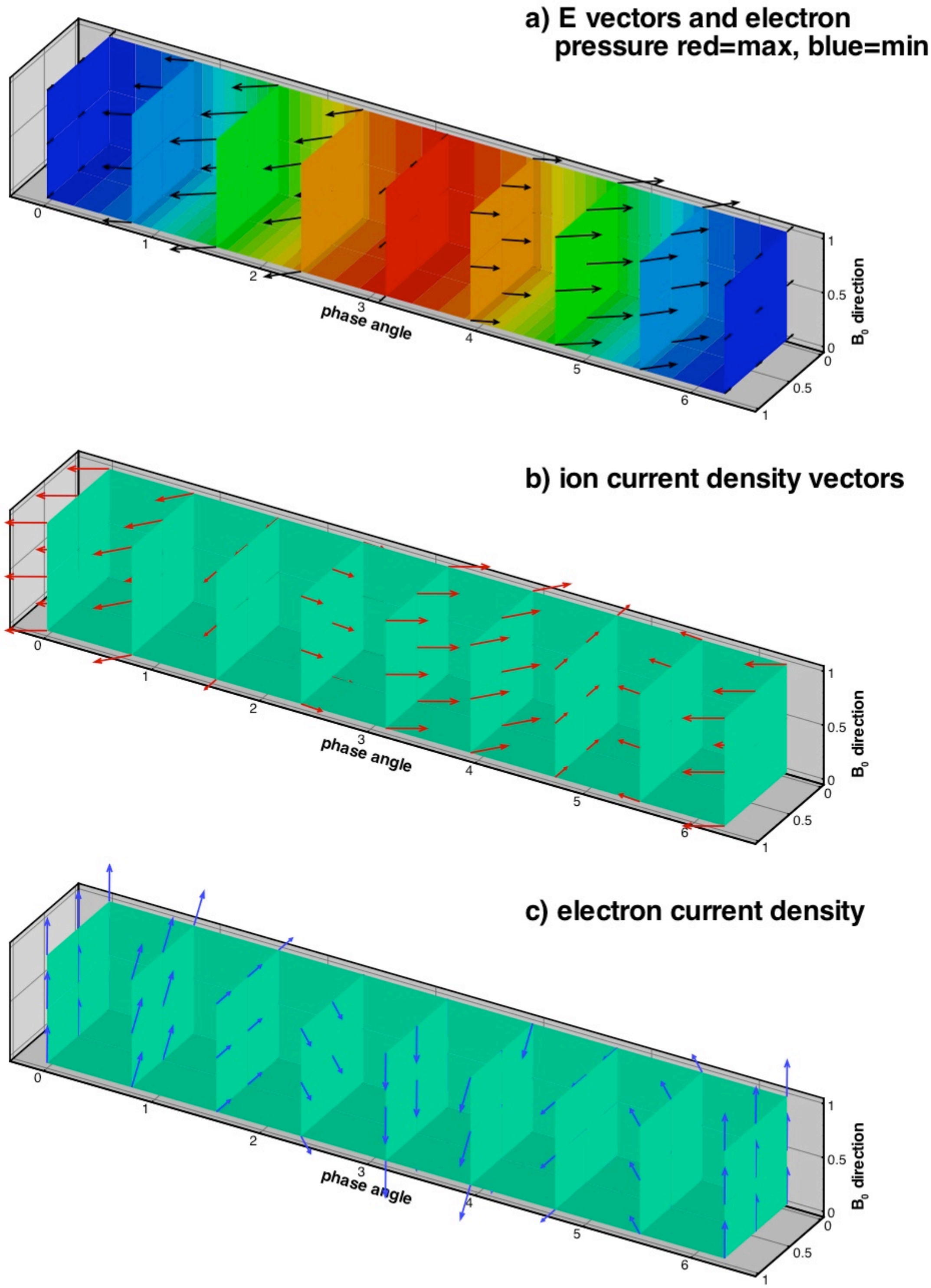

Figure 2. KAW polarization information from the DISPERSION code for $\underline{k} = 19.6$, $\underline{k}_z = 0.31$, and $\beta = 0.64$. Note that the ion current density vectors in b) and the electron current density vectors in c) have separate scales; the ion current density and the *x*-component of the electron current density are about 100 times smaller than the *y*- and *z*- components of electron current density.

This behavior can be compared with the low-frequency limit, $\underline{\omega}^2 << 1$, where ions have $\mathbf{E}\times\mathbf{B}_0$ in the directions perpendicular to $\mathbf{E}$ and polarization drift parallel to $\mathbf{E}$ in the *x-y* plane. The *x*- and *y*-components of (1) are replaced with

$$
\begin{aligned}
v_{i_x} &= \frac{e}{m_i\Omega_i^2}\left(-i\omega E_x + \Omega_i E_y\right) \\
v_{i_y} &= \frac{e}{m_i\Omega_i^2}\left(-\Omega_i E_x - i\omega E_y\right)
\end{aligned}
\qquad (17)
$$

which makes the algebraic system

$$
\begin{pmatrix}
\underline{k}_z^2 - \underline{\omega}^2 & 0 & -\underline{k}_x\underline{k}_z \\
0 & \underline{k}^2 - \underline{\omega}^2 & i\underline{\omega}\dfrac{\underline{k}_x}{\underline{k}_z} \\
-\underline{k}_x\underline{k}_z & -i\underline{\omega}\dfrac{\underline{k}_x}{\underline{k}_z} & \underline{k}_x^2 + 1 - \dfrac{\underline{\omega}^2}{\beta\underline{k}_z^2}
\end{pmatrix}
\cdot
\begin{pmatrix} E_x \\ E_y \\ E_z \end{pmatrix}
=
\begin{pmatrix} 0 \\ 0 \\ 0 \end{pmatrix} \quad . \qquad (18)
$$

Here, currents from electron and ion $\mathbf{E}\times\mathbf{B}_0$ drifts cancel except for the electron drifts that perturb pressure. In this limit, we also have $\underline{k}^2 << 1$, so the dispersion relation from (18)

$$
\left(\underline{k}_z^2 - \underline{\omega}^2\right)\left[\left(\underline{k}^2 - \underline{\omega}^2\right)\left(\underline{k}_x^2 + 1 - \frac{\underline{\omega}^2}{\beta\underline{k}_z^2}\right) - \underline{\omega}^2\frac{\underline{k}_x^2}{\underline{k}_z^2}\right] - \underline{k}_x^2\underline{k}_z^2\left(\underline{k}^2 - \underline{\omega}^2\right) = 0 \qquad (19)
$$

is approximately

$$
\left(\underline{k}_z^2 - \underline{\omega}^2\right)\left[\left(\underline{k}^2 - \underline{\omega}^2\right)\left(\beta\underline{k}_z^2 - \underline{\omega}^2\right) - \underline{\omega}^2\beta\underline{k}_x^2\right] \cong 0 \qquad (20)
$$

when keeping terms that are no more than third order in $\underline{k}^2$, $\underline{\omega}^2$, or combinations of these small factors after multiplying by $\beta\underline{k}_z^2$. The shear wave has $\underline{\omega}^2 = \underline{k}_z^2$, and its eigenvector has $\mathbf{E}$ in the *x*-direction. The transition of the shear wave to the KAW involves the net *x-y* ion current changing from ion polarization in the MHD limit to simple acceleration and suppression of the ion $\mathbf{E}\times\mathbf{B}_0$ drift so that pressure is coupled to electron current.

After getting familiar with the dispersion relations for the $\underline{\omega}^2 >> 1$ and $\underline{\omega}^2 << 1$ limits, it is easier to find the transition from the shear Alfvén wave to the KAW in a more complete model. Keeping the general relation for cold ions, $-i\omega m_i\mathbf{v}_i = e\left(\mathbf{E} + \mathbf{v}_i \times \mathbf{B}_0\right)$, we have the following relation for each component:

$$
\begin{aligned}
v_{i_x} &= \frac{e}{m_i\left(\Omega_i^2-\omega^2\right)}\left(-i\omega E_x+\Omega_i E_y\right)\\
v_{i_y} &= \frac{e}{m_i\left(\Omega_i^2-\omega^2\right)}\left(-\Omega_i E_x-i\omega E_y\right) \quad ,\\
v_{i_z} &= \frac{ie}{m_i\omega}E_z
\end{aligned}
\tag{21}
$$

which becomes (1) in the high-frequency limit and the *x*- and *y*-components become (17) in the low-frequency limit. We will also make the electron model a little more general. Equation (5) is not valid for **k** perpendicular to $\mathbf{B}_0$, and one could ask whether this limiting behavior is related to the KAW transition. Adding electron momentum only to the *z*-component of (4) allows us to cover the range where the electrons become adiabatic. We will not need frequencies anywhere near the electron cyclotron resonance, so leaving electron inertia (polarization drift) out of the *x*- and *y*- components is not inconsistent. Instead of (5), we now have

$$
\begin{aligned}
v_{e_x} &= \frac{e}{m_e\Omega_e}E_y\\
v_{e_y} &= -\frac{e}{m_e\Omega_e}E_x-k_x\frac{\Pi e}{\Omega_e\left(\omega^2-\Pi k_z^2\right)}\left(i\frac{\omega k_x}{m_e\Omega_e}E_y+\frac{k_z}{m_e}E_z\right) \quad .\\
v_{e_z} &= \frac{e}{m_e\left(\omega^2-\Pi k_z^2\right)}\left(\frac{\Pi k_x k_z}{\Omega_e}E_y-i\omega E_z\right)
\end{aligned}
\tag{22}
$$

With the same steps that led from (1) and (5) to (8), combining (21) and (22) into a conductivity relation and using this more general conductivity in the wave equation produces

$$
\begin{pmatrix}
\underline{k}_z^2+K & i\underline{\omega}K & -\underline{k}_x\underline{k}_z\\
-i\underline{\omega}K & \underline{k}^2+K+\dfrac{\beta\underline{k}_x^2}{1-m_i\beta\underline{k}_z^2/m_e\underline{\omega}^2} & -i\dfrac{m_i\beta\underline{k}_x\underline{k}_z/m_e\underline{\omega}}{1-m_i\beta\underline{k}_z^2/m_e\underline{\omega}^2}\\
-\underline{k}_x\underline{k}_z & i\dfrac{m_i\beta\underline{k}_x\underline{k}_z/m_e\underline{\omega}}{1-m_i\beta\underline{k}_z^2/m_e\underline{\omega}^2} & \underline{k}_x^2+1+\dfrac{m_i/m_e}{1-m_i\beta\underline{k}_z^2/m_e\underline{\omega}^2}
\end{pmatrix}
\begin{pmatrix}E_x\\E_y\\E_z\end{pmatrix}=\begin{pmatrix}0\\0\\0\end{pmatrix} \quad ,
\tag{23}
$$

where $K\equiv\underline{\omega}^2/\left(\underline{\omega}^2-1\right)$ represents ion inertia effects. For the *xx*- and *yy*-elements, ion polarization is $K\to-\underline{\omega}^2$ at low frequency. and ion acceleration is $K\to1$ at high frequency. This factor also represents the cancellation of electron $\mathbf{E}\times\mathbf{B}_0$ at low frequency where the *xy*- and *yx*-elements are proportional to $\underline{\omega}^3$.

From the lower-right 2×2 of the matrix in Eq. (23), we see that the equilibration of electron pressure with electric field is a process that is distinct from any other transition. In conditions where $\underline{\omega}^2 >> m_i \beta \underline{k}_z^2 / m_e$, the electrons are not able to equilibrate fast enough. Without displacement current, there are no plasma oscillations, $E_z \cong 0$, and the only physically meaningful wave is the compressional wave. The transition to $\underline{\omega}^2 << m_i \beta \underline{k}_z^2 / m_e$ occurs with a very small parallel component of **k**, because it is an electron thermal process that is evident from the mass ratio appearing with β. Note that in this condition of equilibrated electrons, (23) looks very similar to (8), apart from the ion term K and a term that is proportional to m_e/m_i in the *yy*-element. We conclude that electron equilibration is not part of the transition from the shear Alfvén wave to the KAW; though, it is necessary to have a KAW.

With equilibrated electrons, the dispersion relation from (23) is

$$\begin{aligned} &\underline{\omega}^4 K^2 - \underline{\omega}^2 \left\{ \left(\underline{k}^2 + K\right)\left(\underline{k}_z^2 + K\right) + \beta\left[K\left(\underline{k}_x^2 + K\underline{k}_z^2\right) + \underline{k}_x^2 \underline{k}_z^2 (1-K)^2\right] \right\} \\ &\qquad + \beta \underline{k}_z^2 \left(\underline{k}^2 + K\right)\left(\underline{k}_z^2 + K + K\underline{k}_x^2\right) = 0 \end{aligned} , \tag{24}$$

which limits to Eq. (10) for $K \to 1$ and to Eq. (20) for $K \to -\underline{\omega}^2$ and consistent ordering of small factors. The first term of (24) is important for the fast wave but not the shear Alfvén/KAW branch. For this branch, we have

$$\frac{\underline{\omega}^2}{\underline{k}_z^2} \left\{ \left(\underline{k}_z^2 + K\right) + \frac{\beta}{\left(\underline{k}^2 + K\right)} \left[K\left(\underline{k}_x^2 + K\underline{k}_z^2\right) + \underline{k}_x^2 \underline{k}_z^2 (1-K)^2\right] \right\} - \beta\left(\underline{k}_z^2 + K + K\underline{k}_x^2\right) \cong 0 \quad . \tag{25}$$

At low frequency and dropping second order in $\underline{k}^2$, $\underline{\omega}^2$, or combinations thereof in (25), the shear Alfvén contribution $\underline{k}_z^2 + K$ can be factored. With increasing wavenumber such that $\underline{k}^2$ is not small, $\underline{k}_z^2 + K$ cannot be factored from the last term of (25). Nonetheless, if $\beta \underline{k}^2 << 1$, the frequency remains low, $\underline{\omega}^2 \sim \underline{k}_z^2$. The transition to KAW therefore occurs when $\beta \underline{k}^2 = \beta d_i^2 k^2 = \rho_s^2 k^2$ is approximately unity, which forces the dispersion relation to be a balance between both terms in (25).

A final point is that the KAW is lost at sufficiently large wavenumber. When $\underline{k}_z^2$ is not small, but $\beta \underline{k}^2 << 1$, Eqs. (11) and (12) are both valid and produce the same solutions. The CA wave becomes the whistler, and the KAW becomes the demagnetized sound wave.

Acknowledgment

Thanks go to Slava Lukin for comments on poloidal-β and for helping improve clarity.

References

[1] B. N. Rogers, R. E. Denton, J. F. Drake, and M. A. Shay, "Role of dispersive waves in collisionless magnetic reconnection," Phys. Rev. Lett. **87**, 195004 (2001).

[2] V. V. Mirnov, C. C. Hegna, and S. C. Prager, "Two-fluid instability in force-free magnetic configurations," Phys. Plasmas **11**, 4468 (2004).

[3] G. Schmidt, *Physics of High Temperature Plasmas*, 2nd ed., p. 101 (Academic Press, New York, 1979).